



# Lawrence Berkeley Laboratory

UNIVERSITY OF CALIFORNIA

RECEIVED  
LAWRENCE  
BERKELEY LABORATORY

AUG 29 1983

LIBRARY AND  
DOCUMENTS SECTION

Submitted to Physical Review Letters

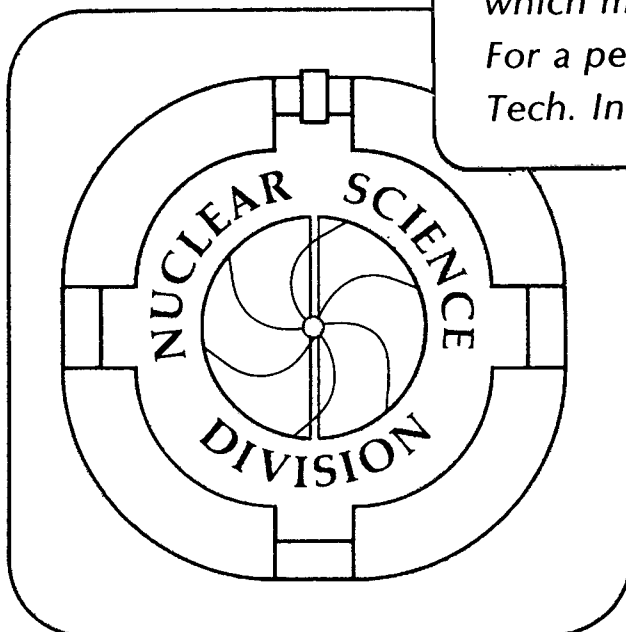
COMPOUND NUCLEUS DECAY VIA THE EMISSION  
OF LARGE FRAGMENTS

L.G. Sobotka, M.L. Padgett G.J. Wozniak,  
G. Guarino, A.J. Pacheco, L.G. Moretto, Y. Chan,  
R.G. Stokstad, I. Tserruya, and S. Wald

July 1983

## TWO-WEEK LOAN COPY

*This is a Library Circulating Copy  
which may be borrowed for two weeks.  
For a personal retention copy, call  
Tech. Info. Division, Ext. 6782.*



LBL-15696  
<sup>2</sup>

## **DISCLAIMER**

This document was prepared as an account of work sponsored by the United States Government. While this document is believed to contain correct information, neither the United States Government nor any agency thereof, nor the Regents of the University of California, nor any of their employees, makes any warranty, express or implied, or assumes any legal responsibility for the accuracy, completeness, or usefulness of any information, apparatus, product, or process disclosed, or represents that its use would not infringe privately owned rights. Reference herein to any specific commercial product, process, or service by its trade name, trademark, manufacturer, or otherwise, does not necessarily constitute or imply its endorsement, recommendation, or favoring by the United States Government or any agency thereof, or the Regents of the University of California. The views and opinions of authors expressed herein do not necessarily state or reflect those of the United States Government or any agency thereof or the Regents of the University of California.

COMPOUND NUCLEUS DECAY VIA THE EMISSION OF LARGE FRAGMENTS

L.G. Sobotka, M.L. Padgett, G.J. Wozniak, G. Guarino, A.J. Pacheco,  
L.G. Moretto, Y. Chan, R.G. Stokstad, I. Tserruya, and S. Wald

Nuclear Science Division  
Lawrence Berkeley Laboratory  
University of California  
Berkeley, CA 94720

This work was supported by the Director, Office of Energy Research,  
Division of Nuclear Physics of the Office of High Energy and Nuclear Physics  
of the U.S. Department of Energy under Contract No. DE-AC03-76SF00098

## Compound Nucleus Decay Via the Emission of Large Fragments

L.G. Sobotka, M.L. Padgett, G.J. Wozniak, G. Guarino,<sup>a)</sup> A.J. Pacheco,<sup>b)</sup>  
L.G. Moretto, Y. Chan, R.G. Stokstad, I. Tserruya,<sup>c)</sup> and S. Wald

Nuclear Science Division  
Lawrence Berkeley Laboratory  
University of California  
Berkeley, CA 94720

## Abstract

The production of  $^4\text{He}$ , Li,  $^7\text{Be}$ ,  $^9\text{Be}$ , B, C, N, O, and F has been studied in the reaction 90 MeV  $^3\text{He} + \text{natAg}$ . The energy spectra, charge and angular distributions indicate that an equilibrium statistical process is responsible for the production of these fragments in the backward hemisphere. The energy spectra exhibit a smooth trend from Maxwellian to Gaussian and the angular distributions evolve from flat to backward peaked as the mass of the ejectile is increased.

PACS 25.70.Gh, 27.60.+j

- a) Permanent address: Università Degli Studi Di Bari, 70100 Bari, Italy
- b) Permanent address: Comisión Nacional de Energía Atómica, Buenos Aires, Argentina
- c) Permanent address: Weizmann Institute of Science, Rehovot 76100, Israel

The typical compound nucleus decay populates two very distinct mass regions. Evaporation produces fragments with masses of four or less, while fission produces fragments close to one-half the mass of the compound nucleus. The mass regions populated are so different that the two decay processes have been generally considered to be also quite different, as indicated even by their names. Such a dichotomy is stressed in the formalisms commonly used to calculate the decay widths. Light particle evaporation<sup>1</sup> is treated by applying the principle of detailed balance to connect the compound nucleus with the residue nucleus plus evaporated particle at infinite separation, whereas the transition state formalism<sup>2</sup> applied at the saddle point is used for fission decay.

Recently, several authors have tried to reconcile these apparently different formalisms to treat the different decay modes of the compound nucleus.<sup>3-5</sup> In particular, the model presented in ref. 3 describes, in a continuous way, the transition from light particle emission to fission. Such a treatment predicts that complex fragments intermediate in mass between  $\alpha$ -particles and fission fragments ought to be emitted with low probability by the compound nucleus. This theory also predicts changes in the shapes of both the kinetic energy spectra and angular distributions of the complex fragments as their masses increase from  $\alpha$ -particles toward fission fragments. These predictions<sup>3</sup> are amenable to experimental test; unfortunately, there is a surprising lack of experimental data that can be compared with the above unified treatments or with more standard formalisms.<sup>6,7</sup>

Complex fragments have been observed in high-energy proton reactions.<sup>8-11</sup> However, the origin of these fragments cannot be easily or unequivocally traced to a well-characterized compound nucleus because precompound processes dominate and multiple fragmentation of the target is possible. Heavy-ion

reactions at low bombarding energies<sup>12</sup> have been shown to produce equilibrated compound nuclei (e.g.,  $^{26}\text{Al}$ ) from which Li or Be nuclei are emitted with low probability. At bombarding energies above  $\sim 8$  MeV/nucleon,<sup>13</sup> however, the fragments of interest are also produced by projectile breakup, thus complicating the study of compound nucleus decay.

In this letter we present experimental evidence for the emission of complex nuclei from helium through fluorine by compound nuclei produced in the reaction  $90 \text{ MeV } ^3\text{He} + ^{\text{nat}}\text{Ag}$ . The specific choice of  $^3\text{He}$  as projectile was dictated by two reasons. First, it is desirable to have a low velocity projectile to minimize preequilibrium losses but massive enough to bring in sufficient energy. Second, the mass of the projectile should be sufficiently smaller than those of the complex fragments of interest to rule out the ambiguity of projectile fragmentation or multinucleon transfer.

The  $^3\text{He}$  beam was produced by the Lawrence Berkeley Laboratory 88-Inch Cyclotron. The atomic number and the energy spectra of the intermediate mass fragments were measured in a set of three standard gas, solid-state ( $300 \text{ } \mu\text{m}$ ,  $d\Omega \sim 1.2 \text{ msr}$ )  $\Delta E$ -E telescopes operated at a pressure of 100 torr. Alpha particles were detected in a separate solid-state telescope ( $40 \text{ } \mu\text{m}$ ,  $5 \text{ mm}$ ,  $d\Omega = 0.35 \text{ msr}$ ). Angular distributions were obtained from  $20^\circ$  to  $170^\circ$  in the laboratory. At forward angles an intense low-energy peak was observed in all light ejectile spectra due to carbon buildup ( $\sim 2 \text{ } \mu\text{g}/\text{cm}^2$ ) on the Ag target ( $2.03 \text{ mg}/\text{cm}^2$ ). Spectra obtained at each angle with a carbon target were normalized and subtracted from the spectra taken with the Ag target to correct for this contamination. This correction is large at forward and small at backward angles. X-ray fluorescence studies of the target showed no significant amounts of heavy element impurities.

To determine the existence of an isotropically emitting source and its velocity, the laboratory energy spectra were transformed into invariant cross-section plots in velocity space which are presented in Fig. 1. In this presentation the velocity of the source is given by the vector that is the center of arcs of constant invariant cross section. The peak cross section for a heavy complex fragment, such as carbon, has a constant value and occurs at the same c.m. velocity from  $170^\circ$  to  $40^\circ$  (as indicated by the position of the X's relative to the circular arc). At the most forward angle the peak cross section occurs at a slightly increased velocity. Similarly, the higher velocity region (the region near the arc with the larger radius) shows no significant change in the backward hemisphere, but does stretch out at forward angles. For a light complex fragment such as Li, the peak of the cross section occurs at a constant c.m. velocity for a smaller backward angle region ( $170^\circ$  to  $120^\circ$ ). Forward of  $120^\circ$  the peak increases both in cross section and in velocity. The slope of the high-energy tail does not change significantly for the three most backward angles, but the intensity of the tail increases as the scattering angle decreases. The  $^9\text{Be}$  and B fragments show a behavior intermediate between that of Li and C. In general, the heavier ejectiles show patterns more consistent with the emission from a single source.

Two conclusions can be drawn from these invariant cross-section plots. First, for all elements there is an angular region in the backward hemisphere where only a single component is observed, which can be characterized by c.m. emission. This angular region increases and extends to more forward angles as the ejectile mass increases. Second, there is a component of non-c.m. emissions that results in harder energy (or velocity) spectra at forward angles.

The energy spectra of the equilibrium component in the c.m. system are shown in Fig. 2. The mean energies of the spectra are Coulomb-like and increase as the charge of the fragment increases. The most interesting feature in the energy spectra of the equilibrium component is the evolution from a Maxwellian shape for  $\alpha$ -particles (not shown) or Li ions through a more symmetric shape for B or C to a symmetric shape for the heaviest ejectiles, as predicted in Ref. 3. In previous high energy proton studies,<sup>10-11</sup> an exponential tail was observed for all ejectiles. This tail, produced by sources other than equilibrium emission from the center-of-mass system, masks the shape of the equilibrium component. At forward angles, our data also show the presence of a nonequilibrium exponential tail.

The experimental yields of the equilibrium component are shown in Fig. 3. To minimize contributions from sources other than the compound nucleus, we have plotted the yields only for the most backward angle ( $171^\circ$ ). These yields drop precipitously in going from  $Z = 2$  to  $Z = 3$ , after which they decrease more slowly. The one exception is the enhanced  $Z = 6$  yield.

Regardless of whether the transition state approach or an evaporation formalism is employed, the yield from an equilibrium statistical emission process should be roughly proportional to a factor  $\exp[-B_Z/T_Z]$ , where  $B_Z$  is the emission barrier for fragment  $Z$  and  $T_Z$  is the temperature at the barrier. More quantitatively, the decay width is given by<sup>4</sup>

$$\Gamma_Z \propto T_Z [E/(E - B_Z)]^2 \exp[2\sqrt{a(E - B_Z)} - 2\sqrt{aE}] \quad 1)$$

$$\propto \exp[-B_Z/T_Z] \quad 2)$$



To calculate the theoretical yields, the following expression for the barrier was used

$$B_Z = U_1 + U_2 + \frac{Z_1 Z_2 e^2}{d} + U_{\text{prox}} - U_{\text{CN}} \quad , \quad 3)$$

where  $U_1$  is the experimental mass of the light fragment,  $U_2$ ,  $U_{\text{CN}}$  are the droplet model masses of the residual and compound nucleus, respectively, and  $U_{\text{prox}}$  is the proximity potential. The center-to-center distance  $d$  in the interfragment Coulomb term was taken to be  $d = 1.225(A_1^{1/3} + A_2^{1/3}) + 2$  fm. The addition of 2 fm was done to obtain rough agreement with the energy spectra.

The temperature ( $T_Z$ ) was evaluated using  $E - B_Z = aT_Z^2$ . A compound

nucleus excitation energy ( $E$ ) of 102 MeV (the value for full momentum

transfer) and a level density parameter ( $a$ ) of  $A_2/8$  were assumed. The cal-

culated yields (Eq. 1) for each isotope were multiplied by  $2I + 1$  (where  $I$  is the ground state spin of the light fragment) and then summed. The theoretical

ejectile yields were calculated as a ratio  $\Gamma_Z/\Gamma_6$  and have been normalized

to the data at  $Z = 6$  in Fig. 3.

The agreement between the data (circles) and this simple equilibrium statistical calculation (solid line) is exceptionally good for  $Z = 3-9$ . The calculation underpredicts the  $\alpha$ -particle yield because it only takes into account first chance emission, whereas substantial amounts of higher chance  $\alpha$ -emission occur. Precompound emission is expected to leave the compound nucleus with a broad excitation energy distribution with a most probable value<sup>14</sup> of  $\sim 85$  MeV. A calculation (not shown) with this lower excitation energy also reproduces the relative yields of the heavy fragments quite well but overpredicts the yield of first chance  $\alpha$ -emission. More detailed comparisons between the data and theory require calculations that include

precompound emission; however, the substantial agreement depicted in Fig. 3 does indicate that an equilibrated process is responsible for the emission of these complex fragments.

The angular distributions in the center of mass are shown in Fig. 4. From  $\sim 100^\circ$  to  $180^\circ$  the angular distributions change from flat to backward peaked as the ejectile mass increases. Such an increase in anisotropy with increasing particle mass is well understood from angular momentum considerations and discussed in some detail in ref. 3. These angular distributions, which for the heaviest elements have a minimum at  $\sim 90^\circ$ , are consistent with an equilibrium process for the complex fragments observed in the backward hemisphere.

In summary, we have observed the emission of large fragments (He to F) from the reaction  $90 \text{ MeV } ^3\text{He} + \text{natAg}$ . Various aspects of these data suggest that these complex fragments are emitted from an equilibrated compound nucleus. At backward angles the fragment energies are Coulomb-like. A single source with the c.m. velocity is observed in the invariant cross-section plots. As the charge of the ejectile increases, the yield decreases nearly exponentially, the angular distributions evolve from flat to backward peaked, and the energy spectra evolve from Maxwellian to Gaussian.

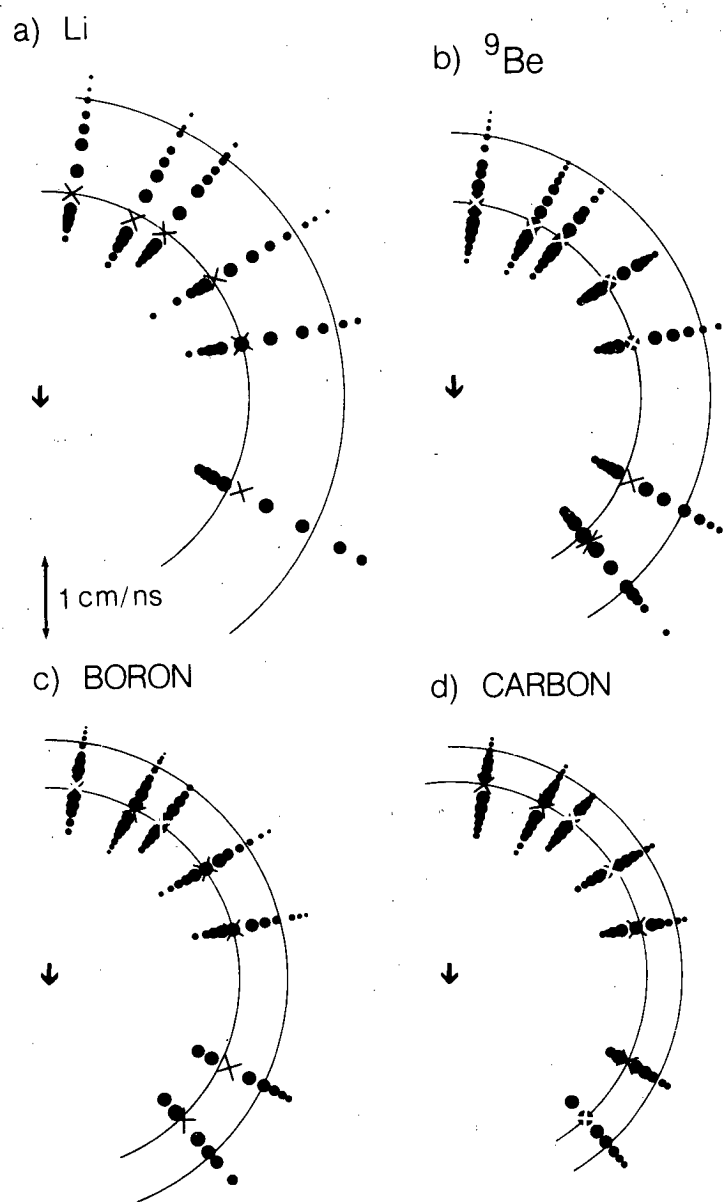
This work was supported by the Director, Office of Energy Research, Division of Nuclear Physics of the Office of High Energy and Nuclear Physics of the U.S. Department of Energy under Contract DE-AC03-76SF00098.

## References

1. V.F. Weisskopf and D.H. Ewing, Phys. Rev. 57, 472 (1940).
2. J.A. Wheeler, "Channel Analysis of Fission" in Fast Neutron Physics Part II, ed. J. B. Marion (Interscience Publishers, New York, 1963), p. 2051.
3. L.G. Moretto, Nucl. Phys. A247, 211 (1975).
4. W.J. Swiatecki, Lawrence Berkeley Laboratory Report LBL-11403 (to be published, Australian J. of Phys.).
5. D.N. Poenaru, M. Ivascu, and A. Sandulescu, J. Phys. G5, L169 (1979).
6. T. Ericson, Advan. Phys. 9, 425 (1960).
7. T.D. Thomas, Ann. Revs. Nucl. Sci. 18, 343 (1968).
8. E. Baker et al., Phys. Rev. 112, 1319 (1958).
9. I. Dostrovsky et al., Phys. Rev. 118, 781 (1960).
10. G.D. Westfall et al., Phys. Rev. C17, 1368 (1978).
11. R. Green and R. Korteling, Phys. Rev. C22, 1594 (1980).
12. D.L. Hanson et al., Phys. Rev. C9, 929 (1974).
13. R.G. Stokstad et al., Phys. Rev. C16, 2249 (1977).
14. M. Blann, private communication (1983).

## Figure Captions

- Fig. 1. Invariant cross-section plots  $\left( \propto \frac{1}{v^2} \frac{d^2\sigma}{d\Omega dv} \right)$  for representative ejectiles (Li,  $^9\text{Be}$ , B, and C). The diameter of the dots is proportional to the logarithm of the cross section and the X's indicate the peak of velocity distribution. The two large arcs are sections of circles centered on the c.m. velocity (center arrow) appropriate for complete fusion. The beam direction ( $0^\circ$ ) is indicated by the c.m. velocity vector.
- Fig. 2. Energy spectra in the c.m. system for various ejectiles detected at  $\theta_{\text{c.m.}} = 171^\circ$ . Before correction for carbon contamination the lower level threshold varied from 4 to 12 MeV in the c.m. for Li to O ejectiles, respectively.
- Fig. 3. Experimental (circles) and theoretical yields versus ejectile atomic number (Z).
- Fig. 4. Angular distributions in the c.m. system for various ejectiles. The curves through the data points are to guide the eye. Statistical error bars are only shown when they exceed the size of the data point.



XBL 834-1507

Fig. 1

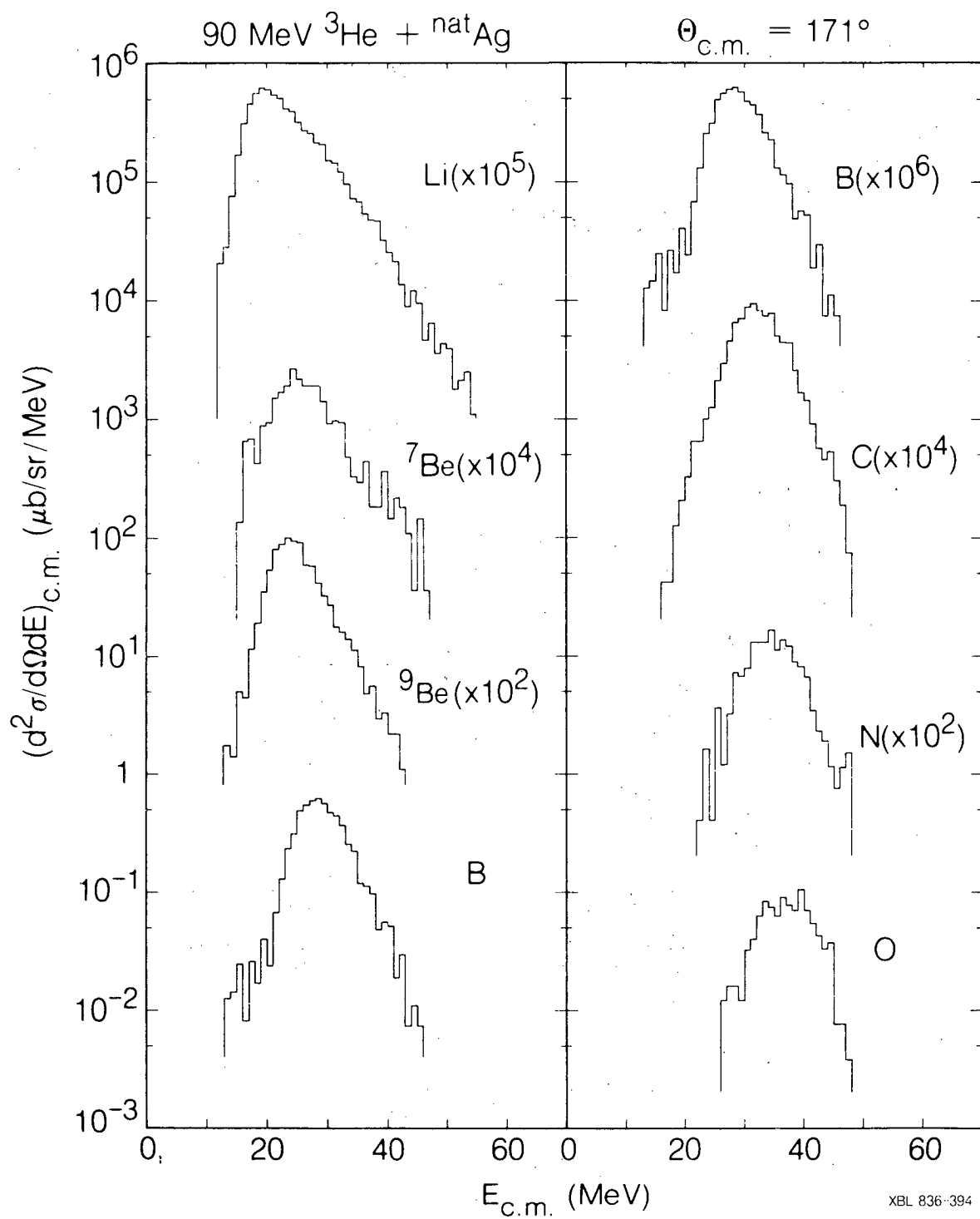
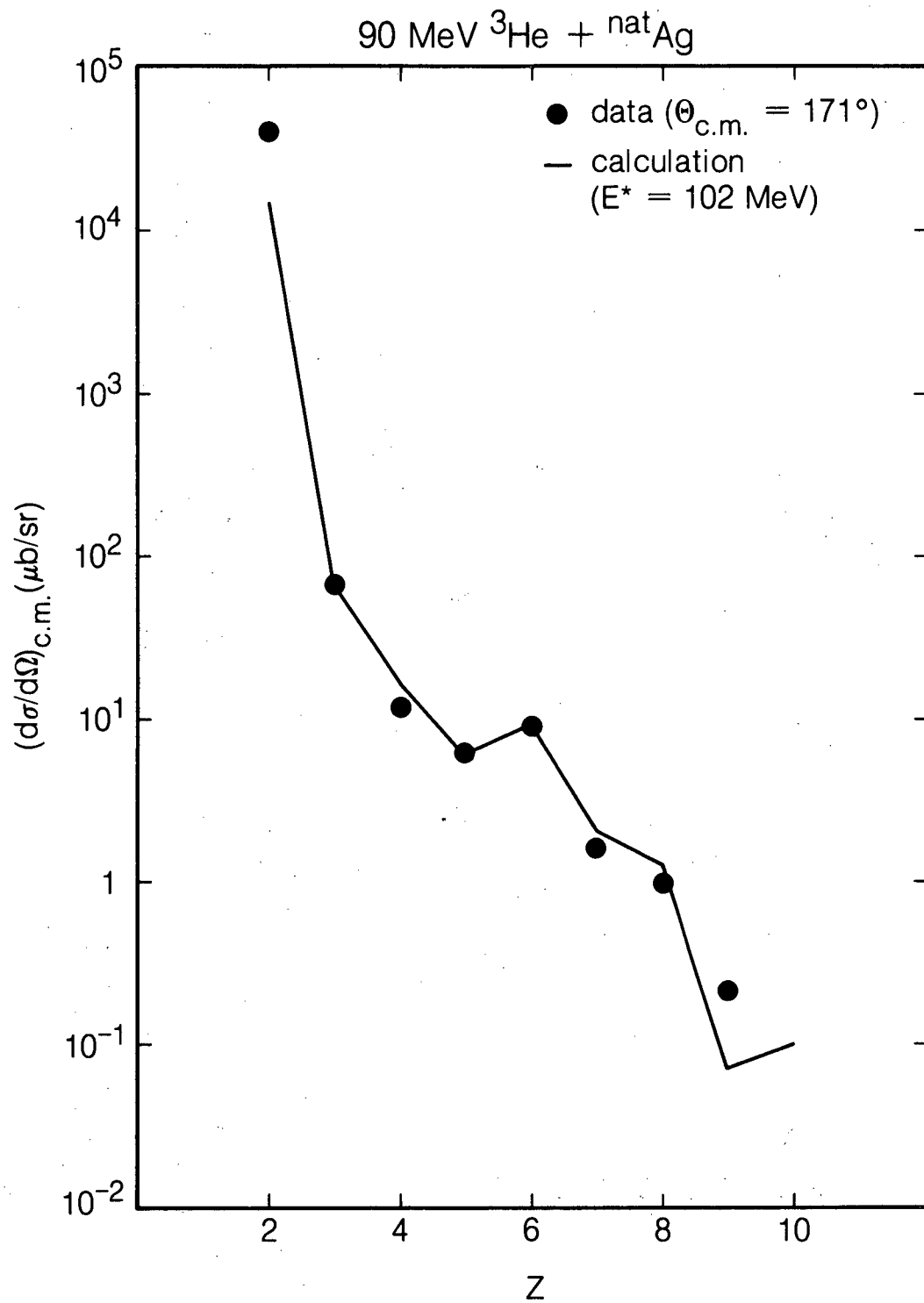
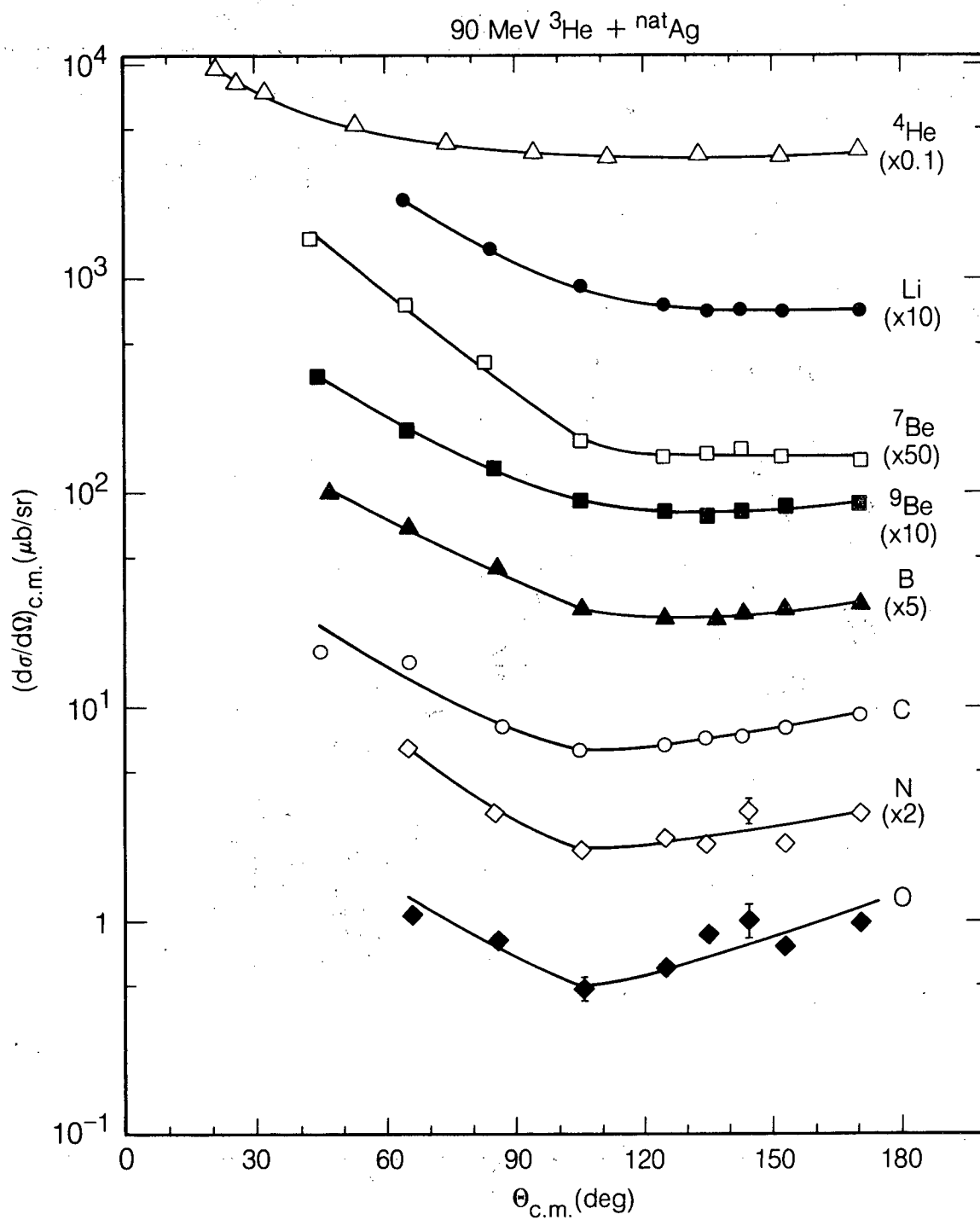


Fig. 2



XBL 836-392

Fig. 3



XBL 836-393

Fig. 4



This report was done with support from the Department of Energy. Any conclusions or opinions expressed in this report represent solely those of the author(s) and not necessarily those of The Regents of the University of California, the Lawrence Berkeley Laboratory or the Department of Energy.

Reference to a company or product name does not imply approval or recommendation of the product by the University of California or the U.S. Department of Energy to the exclusion of others that may be suitable.

TECHNICAL INFORMATION DEPARTMENT  
LAWRENCE BERKELEY LABORATORY  
UNIVERSITY OF CALIFORNIA  
BERKELEY, CALIFORNIA 94720